

See discussions, stats, and author profiles for this publication at: <https://www.researchgate.net/publication/274815653>

A Soft Matter State of Water and the Structures it Forms

Article in *Forum on Immunopathological Diseases and Therapeutics* · January 2012

DOI: 10.11615/ForumImmunDisTher.2013007847

CITATIONS

12

READS

955

4 authors, including:



Alpha Lo

University of Washington Seattle

2 PUBLICATIONS 17 CITATIONS

SEE PROFILE



Shui Yin Lo

126 PUBLICATIONS 750 CITATIONS

SEE PROFILE

A Soft Matter State of Water and the Structures it Forms

Alpha Lo,^{1*} John Cardarella,² Jacob Turner,² & Shui Yin Lo¹

¹Quantum Health Research Institute, Pasadena, CA, USA; ²D&Y Labs, USA

*Corresponding author: Alpha Lo, Quantum Health Research Institute, Pasadena, CA, alplo@yahoo.com

ABSTRACT: Previously solid-like stable water clusters have been found to exist at room temperature as a residue from evaporation of a type of pure water. We examined the behavior of the stable water clusters. They form straight rods, double-helix shapes, and a variety of other structures. Their properties suggest that the water is a soft-matter state with gel-like behavior. Dipole–dipole models with soft-matter properties are presented to explain how many of these structures are created.

KEY WORDS: Water, stable water clusters, soft matter, gel, double helix, dipole, self-assembly

ABBREVIATIONS: **AFM:** atomic force microscopy; **TEM:** transmission electron microscopy

I. INTRODUCTION

Traditionally, there are three known states of matter of water: gas, liquid, and solid. There also exist states between solid and liquid called the soft-matter states: gels, liquid crystals, colloids, emulsions, and polymers.^{1–3} Examples include the cytoplasm, blood, connective tissue, smoothies, and rubber. Lo discovered a form of pure water in which the small clusters of solid-like water coexist inside liquid water.⁴ These clusters, originally called I_E clusters and found to display immunological⁵ and enzymatic effects,⁶ occur in water prepared through a process of repeated dilution of water with charged ions initially contained in it.⁷ It was originally proposed that the solid-like stable water clusters were an anomalous state of ice with a rigid structure.

In this study, we investigated whether the properties the stable water clusters exhibit are gel-like, and whether these properties

indicate that they are a form of soft matter. Such information furthers current research by providing a foundation of the physical properties and behavior of stable water clusters, and it may provide insight into their biological effects. Here, we focused on a specific form of water called “Double Helix Water,” which has evolved incrementally from the original I_E water to contain a greater concentration of stable water clusters. Double Helix Water samples were evaporated to leave a residue which was studied by atomic force microscopy (AFM) and transmission electron microscopy (TEM). A wide range of stable water cluster structures were observed in the residue, including balls, rods, arrays, loops, wreaths, and double-helix shapes.

In section III-A, we present the results of our examination of the structures and behavior of the rods, and we present our inferences about their properties. In section III-B, we propose, based on these inferred

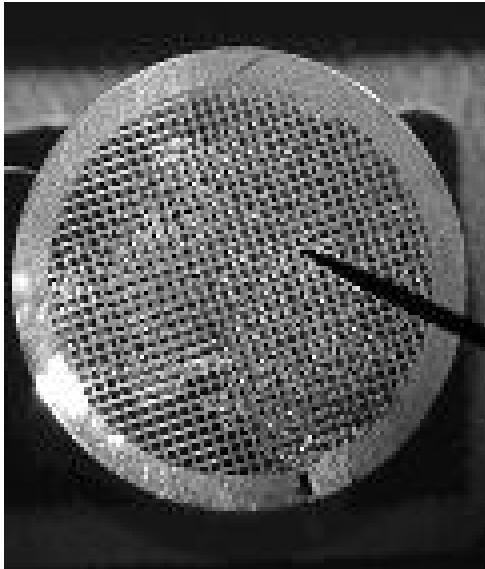


FIG. 1: TEM copper mesh viewed under an optical microscope.

properties, that the stable water clusters are a form of soft matter. We also examined the gel-like behavior of the stable water clusters. In section III-C, we propose a simple coarse-grained model of a malleable rod based on dipoles that naturally leads to the double-helix shape observed in our experiments. In section III-D, we propose a model based on ball dipoles in conjunction with a malleable ambient material that can explain the other types of structures observed.

II. MATERIALS AND METHODS

All samples were prepared in a Class 1000 clean room and were dried under room temperature.

A. Sample Preparation and Imaging for Transmission Electron Microscopy

Double Helix Water droplets of varying vol-

umes from 0.05 to 0.25 ml were placed onto a copper grid (300 mesh) pre-coated with holey thick carbon and evaporated in air at room temperature. The resulting residue was placed under the transmission electron microscope (TEM) for imaging. A Titan T/SEM (80–300 kV) and a CM 120 (120 kV) TEM were used. Darker areas in the image occurred because electrons fired by the TEM were diffracted by the sample. Lighter areas occurred because electrons fired by the TEM were transmitted through the sample.

B. Sample Preparation and Imaging for Atomic Force Microscopy

Double Helix Water droplets of varying volumes were placed on a highly-ordered pyrolytic graphite substrate (Bruker International model HOPG) and evaporated in atmosphere at room temperature. The resulting residue was analyzed using an Innova atomic force microscope (AFM). A Bruker MPP-11100-10 tip was used. Images were then cosmetically treated using built-in software to remove background artifacts.

Given different droplet volumes of 0.05–0.25 mL, different drying times were necessary at the temperature of 20°C in the laboratory. Using a built-in camera on the Innova, dryness was judged by general light diffraction on the residue. High diffraction correlated with the presence of moisture and a need for further drying. Because the contact mode in the AFM can leave an indentation line when the tip is dragged across it, the images in Figure 5 are made with the AFM in tapping mode, which yields contour height information, the contour height being the height of the sample above the substrate. By tapping, the phase information, which reflects changes

in viscoelasticity, adhesion, and contour slope, was recorded. The frequency was tuned to the range 200–400 kHz (average 300 kHz), and a tapping amplitude as measured by the Veeco Innova was 4 V. The tip was engaged to a set point of 65% of the original tapping amplitude (2.6 V). The resolution of the pictures taken was 1024×1024, most often at a size of 5 μm . Scans were conducted at speeds ranging from 0.1 to 0.3 Hz.

III. RESULTS AND DISCUSSION

The following TEM and AFM images represent common features found through the hundreds of images. Notably, these features persisted over a month-long period, suggesting the general stability of the structures compared to typical ice structures. In the TEM images, the white ovals are the holes in the holey thick carbon. The CM120 TEM was used to take the images in Figures 2 and 3. The Titan TEM was used to take the images shown in Figure 4.

A. Structures and Properties of the Rods

In a previous report by Lo, TEM pictures showed that the rods are made of ball-like structures (Figure 6).⁴ The pictures are taken by first coating the rods with a carbon film, then dissolving the water clusters and the filter paper on which they were located, and then using the TEM to image the carbon film. The ball-like structures are lighter than the shell because the carbon film is thinner on the presumed sloped surface of the ball. Direct imaging of the sample with the TEM in this investigation shows the rod being fully dark in Figure 2A. Although we cannot see ball-like structures in Figure 2A, it is assumed that the

ball-like structures are still there, although we acknowledge some small changes in the water preparation from the I_E clustered water preparation. The TEM measures the electrons that are transmitted through the sample. The darkness of the image depends on how many of the electrons are diffracted, which in turn depends on the thickness (height above paper) of the sample, density of the material, the state the matter it is in, and the electric fields generated by the material. The AFM image in Figure 5A, which appears to be two rods joined end to end, gives the contour height of the rod as approximately 500 nm, so the rods are probably several ball-like structures thick. The layers of ball-like structures diffract the electrons, leaving an image of a level of darkness such that we cannot see the patterns of the paper underneath.

The earlier work of Lo has provided some insights into the energies that are holding the structure together.⁸ His previous experiments, which investigate sodium phosphate crystallization in a non-isomorphic manner during the evaporation of stable water clustered water with and without applied electric fields, and measurements of the electromotive force of the water, revealed that the stable water clusters were generating an electric field. Because water itself does not have a net charge, Lo sought to discover what could be causing the field. The hypothesis was that the ball-like structures were dipoles, as dipoles have no net charge but do have positive and negative ends and are thus able to generate an electric field. The most stable configuration of one column of dipoles is if they are parallel. If there is a second column, then that column would be antiparallel to it. The most favorable configuration for arrays of dipoles are in a rod shape, as contrasted with a spherical or any other form. Two rods, if their

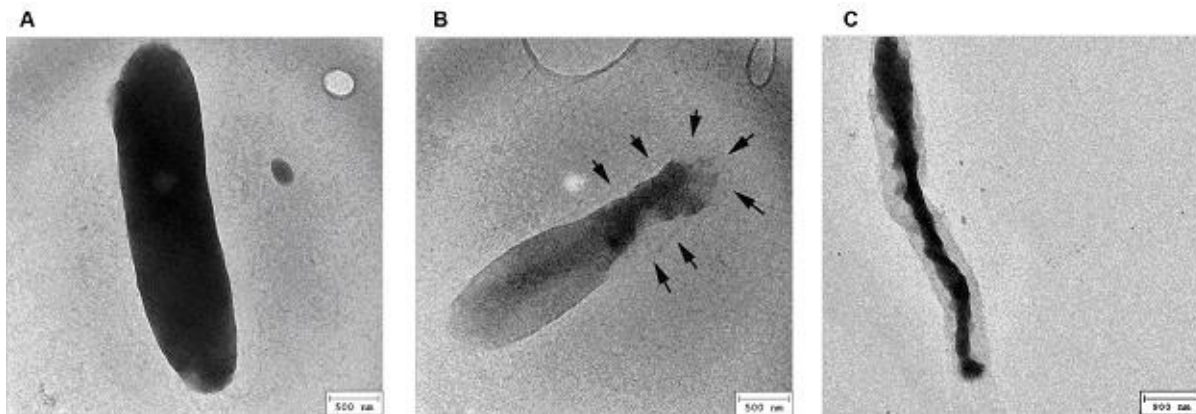


FIG. 2: TEM images (from the CM120) of rods in various forms of darkness. Dark areas correspond to those areas where electrons are not transmitted through the sample, due to diffraction. **(A)** A fully dark rod where the dark area probably corresponds to ball-like structures (shown in Figure 6). The width is ~ 900 nm, length $3.5 \mu\text{m}$; such rods range from 600 to 900 nm. This image does not indicate the thickness, which is ~ 500 nm for a different rod measured by the AFM in Figure 5A. **(B)** A rod with a dark core of smaller size than the outer shell. The faint image of the shells is outlined by arrows. **(C)** Rods have a dark cylinder inside and an electron-translucent shell. The horizontal line halfway along its length indicate that this consists of two rods lined up end to end. Hypothesis: Rods can evolve from shape A to shape B to one of the rod shapes in panel C. Malleable ball-like dipole structures (like those in Figure 6), which initially fill the whole rod in A, are compacted into a cylinder shape in panel C. Note: The level of darkness depends on the voltage of the electrons shot into the sample. When using the Titan TEM, which has higher voltage electrons, the dark areas were more translucent than the same areas shown in the CM120 TEM images.

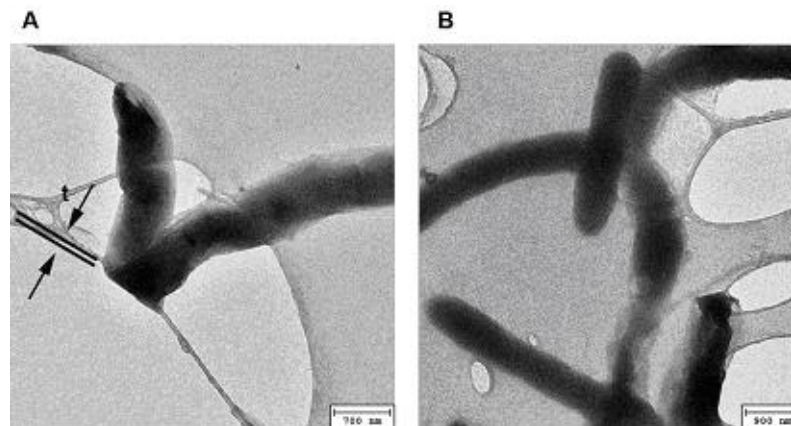


FIG. 3: TEM of rods. White areas are holes in carbon paper. **(A)** Rod folded over a hole in the carbon paper, with part of it on the underside (the image is looking down on the paper). The thickness t of the rod at the bent area is < 100 nm. The thickness of the rod when lying flat on the paper is the height of the rod above the paper. From Figure 5A, we assumed the rod was ~ 500 nm thick. Hypothesis: The material in rod flowed away from the bent area downward due to gravity. **(B)** Rods are present in straight and slightly curved forms, possibly able to flex between forms (i.e., from panel A we know that rods can bend).

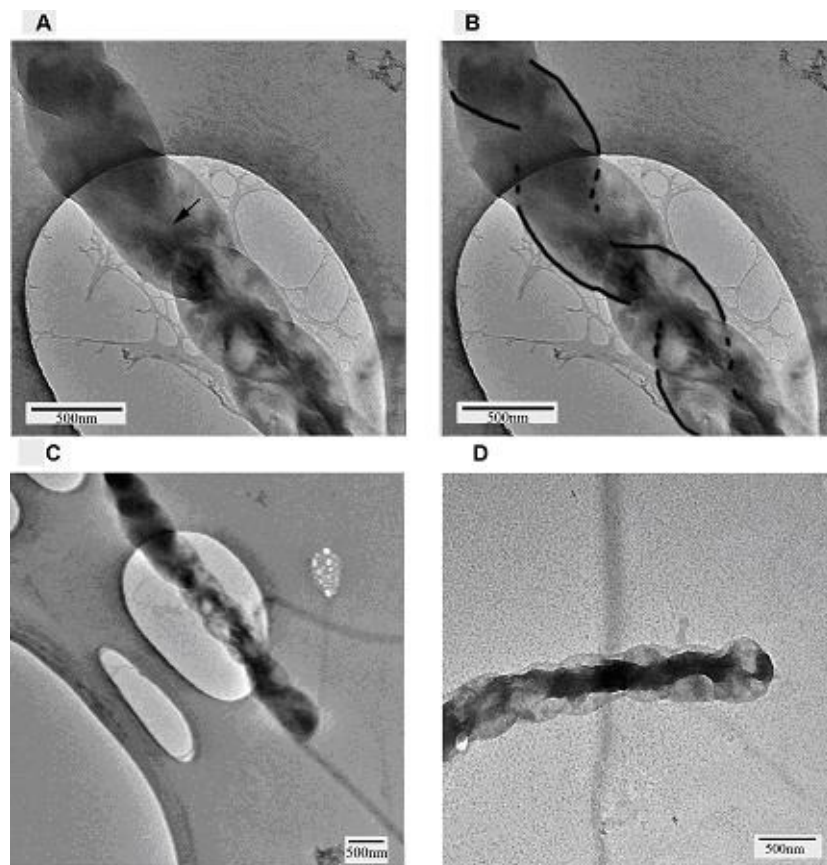


FIG. 4: TEM. Panels **A**, **B**, and **C** are the same image at different scales. The helical structure here is similar to that seen in Figure 5E. **(A)** Two strands are shown, one on either side of the cavity (indicated by an arrow). **(B)** An outline of the two strands winding in double helix. **(C)** A less magnified image of **A**. It is more tightly wound at the ends than in middle. Because the cavity is yet fully wound in the middle, we are able to see the cavity in **A**, which makes the shape discernible as a double helix. **(D)** Another double-helix shape. It has a dark cylinder along the longitudinal axis, but is translucent (to electrons) on the outside. Our hypothesis is that the rods composed of ball-like dipole structures, like those seen in Figure 6 and Figure 2A, wind into double-helix shapes due to the dipole-dipole interaction between the two different rods.

dipoles are aligned, will find one energetically favorable state to be aligned end to end, as shown in Figure 5A.

An examination of the TEM and AFM data reveal intriguing behavior when contrasted with how we normally expect ice or liquid water to behave. Following are some observations and inferences regarding our results: (1)

The rods are able to maintain their form, and have a definite boundary. This is a solid-like property. (2) The rod is folded over the edge of hole in the carbon filter paper (Figure 3A). This suggests that the rods are pliable and able to bend. (3) The lower half of the rod remains on the bottom of the filter paper when it is viewed a day later. This suggests that

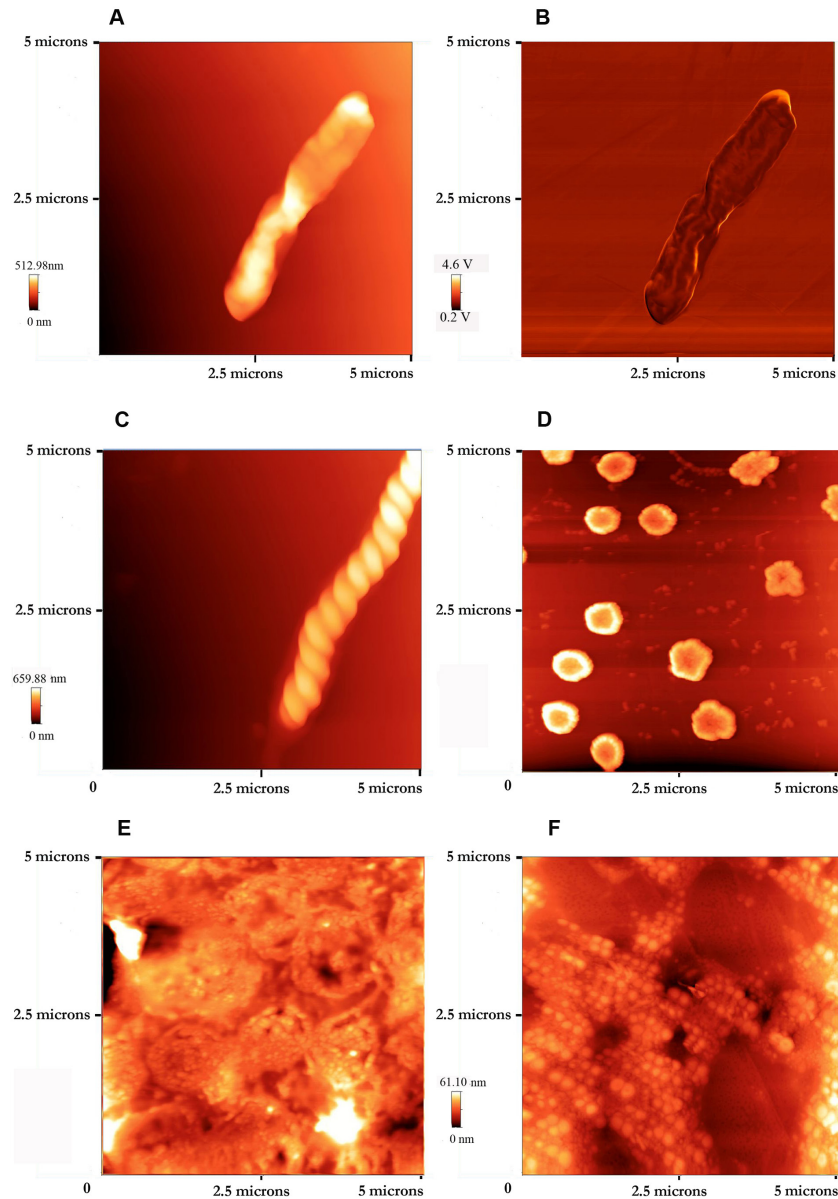


FIG. 5: AFM images. Panels A, C, D, E, and F are contour height maps. Panels D, E, and F have structures made of small ball-like forms, hypothesized previously to be dipoles. (A) Two rods end to end. Contour height reaches ~500 nm. The lower rod resembles the one shown in Figure 2B. The upper rod appears to have two columns, likely made of ball-like structures. (B) Phase image on the same scan as panel A. The phase reflects the viscoelasticity, adhesion and contour slope. (C) The helix structure is hypothesized to be a double helix because it has the same form as that in Figure 4C. (D) Loop structures: In the upper shapes, the small ball-like forms make up the loop. (E) Wreath structures are made of small ball-like forms. (F) In these array structures, the long-range order may be from a dipole electric field of ball-like forms aligning particles. Note the ambient material around the ball-like forms.

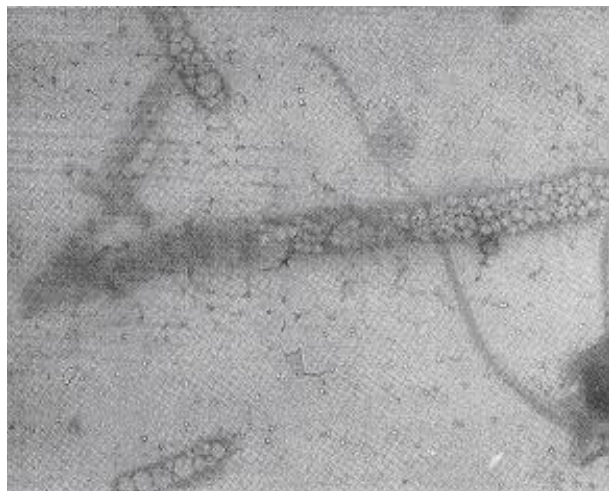


FIG. 6: Reprinted from a previous experiment by Lo.⁸ 6000x magnification. TEM of carbon film on rods, made by spraying carbon film on water clusters, then dissolving the clusters. The largest rod in the center of the image is ~3 balls wide. The rod in the lower left corner of the image is mostly one ball wide.

the rods have a self-supporting structure. (4) The rod is thin and flat where it is draped over the hole (Figure 3A). From the contour height information shown in Figure 5A, we infer that these rods are not flat in general. This suggests that the material from the bent region has flowed down into the bottom half of the rod. Because of the solid-like nature of the rod, this flow would probably be slow, viscous, and limited in extent. (5) Some of the rods are in a straight orientation, some of the rods are in a slightly curved orientation shown in Figure 3B. This suggest that the rods are able to flex, consistent with inferences drawn from Figure 3A. (6) The stable water clusters have sometimes been damaged when the AFM tip in the contact mode is dragged across it, leaving a wide line. This suggests that the stable water clusters are somewhat soft. It is common for soft matter and biological matter to be deformed when

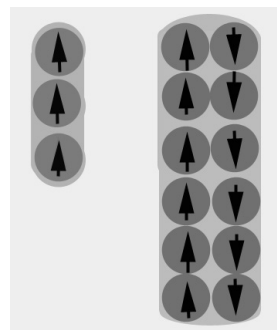


FIG. 7: Configuration of ball dipoles inside a rod. In the one-column rod on the left, dipoles align end to end and are parallel. In the rod on the right, dipoles in different columns are antiparallel.

using the contact mode with the AFM. (7) The ball-like structures inside the rod are observed to be round and in other instances to appear to squish to fit in next to each other compactly. This suggests that the ball-like structures are malleable (Figure 8). (8) The tapping mode will reproduce the same AFM image when run again. This suggests a degree of resiliency of the material to the pressure of the tip on the material. (9) There was no crystalline diffraction pattern observed in any TEM pictures. This suggests that the stable water clusters are amorphous. (10) Figure 2 shows the rods with varying areas of darkness inside: fully dark (Figure 2A) to half dark (Figure 2C). We use the term darkness as a relative term regarding contrasting areas of the image. We assume that the fully dark rod corresponds to it being fully composed of ball-like structures, similar to those seen in Figure 6. The question then arises: What is happening in the material when the darkness is shrunk to a cylinder in Figure 2C? One possibility is that the dipolar ball-like structures have been compacted and are undergoing a volume-phase transition. Generally speaking,



FIG. 8: Reprinted from Lo (80,000x magnification).⁴ Carbon film TEM of a rod. The ball-like structures in the rod appear to be compacted next to each other. A comparison with the round ball-like structures shown in Figure 6 suggests that the balls may be malleable.

solids and liquids are incompressible, so how could the internal structure decrease in size? We can answer this question by considering that, if a solid contains air, it can compress by expelling the air. Similarly, if a solid contains a liquid, it can compress by expelling the liquid. It can thus be hypothesized that the ball-like structures are made of a solid part and a liquid, both made of H₂O molecules. The solid part can hold onto the liquid water until it is under enough pressure to expel the liquid. It is a possibility that the liquid does not have a strong a dipolar nature as the solid part, which will then affect its ability to diffract the TEM electrons.

Lo has suggested that neighboring columns of ball-like structures in a rod have antiparallel dipoles to minimize the electromagnetic potential energy.⁴ We propose here that these neighboring columns may find it energetically favorable, in a manner similar to that discussed in section IIIC (i.e., the double-helix section), to wind into a helical shape. Figures 2B and 5A may represent a picture of this internal structure in the

process of winding. The winding creates compression energy and an osmotic pressure that then expels the liquid water out of the ball-like structures, leading to a compacting of the structure. This ability to expel water is common to a number of gels. These gels are able to undergo volume-phase transitions from a high-volume water-filled state to a dry, low-volume, contracted state, either by expelling liquid or absorbing liquid.^{9,10} The phase transition may be induced by a change in mechanical pressure, composition of solvent, temperature, pH values, irradiation by light, or electric field strength.

B. Soft Matter and Gel-Like Characteristics

The properties inferred in the previous section, which include that of malleability, pliability, a degree of softness, limited viscosity coupled with a general ability to hold its own form, suggest that the state of matter of the stable water clusters is neither liquid nor solid, nor glass,^{11,12} but rather that of the soft-matter state, which is a somewhat loosely defined state dealing with a matter intermediate between solid and liquid that is softer than hard rigid solids or glass. These structures are often easily deformable by external stresses and electromagnetic fields. Soft matters often have interesting structures and self-assembling behavior at the mesoscopic scale.³ The prototypical example of a gel is Jello[®], which is made from collagen. It is soft, deformable, elastic, resilient, made largely of water yet solid-like. There are a number of definitions, of varying generality, of a gel.^{13–18} Almdal *et al.* wrote in “Towards a Phenomenological Definition of the Term Gel” that a gel is (1) soft, (2) solid or solid-like, and (3) consists of

two or more components, one of which is a liquid, present in substantial quantity.¹³ They wrote “A solid has by definition a definite shape. This means that a deformed solid body returns to its original shape after removal of the deforming force.” More precisely, by “solid-like” they meant that this resilient and elastic behavior occurs on time scales up to a few seconds, while on longer time scales the material can have a viscous flow. Technically, this was expressed by Almdal *et al.* as having “a storage modulus $G'(\omega)$ which exhibits a pronounced plateau extending to times at least of the order of seconds, and by a loss modulus, $G''(\omega)$ which is considerably smaller than the storage modulus in the plateau region.”

The first two properties of soft matter and solid or solid-like matter are rheological. The third property, “consisting of two or more components, one of which is a liquid present in substantial quantity,” is a structural property. In regard to the first property, the data led us to reason that the stable water cluster rods are pliable, durable, with slow, viscous flow of limited extent, and deformable to the touch of the AFM tip in the contact mode. This suggests that the stable water cluster rods are soft. In regard to the second property, if “solid-like” is taken to mean that the material has a definite shape, then the rods also have the property of being solid-like. If “solid-like” is taken as the more technical of Almdal *et al.*'s definitions, more experimental data would be required to make the determination. Concerning the third property, if the hypothesis explaining the volume transition of the ball-like structures, which entails in part the ball-like structures being composed of a solid and liquid, is true, then the stable water cluster rod will also have the gel-like property “consisting of two components, one

of which is a liquid present in substantial quantity.” If this hypothesis is true, it can be argued that the stable water cluster rods fit Almdal *et al.*'s definition of a gel.

A number of possible phenomena and models are mentioned here, as they may have relevance to understanding the soft-matter state of water. Zheng and Pollack discovered a form of liquid water which has properties near certain types of surfaces, which they call EZ water. The liquid water excludes microspheres of a certain size from getting near the surfaces.¹⁹ EZ water has a higher viscosity than is normally measured in water. Pollack postulates that the liquid water inside gels are structured in the form of this EZ water.²⁰ EZ water has not yet been found to leave a solid-like residue when evaporated, unlike stable water clusters. If the ball-like structures in the rods are a gel and are made of a solid and a liquid part, it is possible that the liquid part is EZ water and that the ambient material around the ball-like structures is EZ water. Water bridges are phenomena that occur when two beakers of de-ionized water, exposed to high voltages, form a floating bridge between them.²¹ The bridge does not collapse under gravitational forces. Thus, it exhibits both solid-like and liquid-like properties. Del Giudice *et al.* postulated that interactions between the quantized electromagnetic radiation field and the electric dipole of the liquid water lead to the emergence of collective modes and the creation of stable, quantum coherent domains (CDs) approximately 100 nm in size in the liquid water.²² Del Giudice *et al.* proposed that the quantum coherent domains can help explain EZ water and water bridges.²³

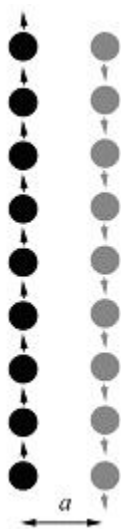


FIG. 9: Two rods simplified as point-like dipoles on one-dimensional lines that are distance a apart. Arrows indicate vector direction of dipoles.

C. Double Helix

Upon closer inspection of Figures 5B and 5C, it is possible to identify two rods forming a double helical structure; the contours of the structure are highlighted in Figure 5C. Figure 5A shows an internal cavity, suggesting that these structures do not result from a single rod forming a spiral structure.

Comparison of the TEM picture in Figure 4A and the AFM picture in Figure 5C shows them to be of the same type of structure, although in the middle of the structure in Figure 4A the helices are not wound as tightly. Therefore, we infer that Figure 5C is also an image of a double-helix shape. In Figure 5C, the rods rise above the paper ~ 600 nm. In Figure 4A, the width of the double-helix is ~ 600 nm. Notably, there is a picture of the double helix in the “Survey of I_E clusters” paper⁸ published 15 years ago, but it was not recognized as such, and the helical

nature of the stable water cluster is not readily discernible from the image. It seems reasonable to conclude that the strands that wind around each other come from the straight rods, as shown in Figure 2A. (Note: The terms “strand” and “rod” are used interchangeably.) The reason the width decreases may be either that the rods stretch and lengthen or that the volume of the rods decreases as they expel water.

Calculations suggest that the rods show electromagnetic potential energetic preference to be in the double helix state. The rods can thus self-assemble into a double helix configuration. The width of the straight rods ranged from 500 to 900 nm. The width of the strands in the helical structure ranged from 200 to 300 nm. To simplify this, the following assumptions were made: (1) Only dipole–dipole interactions between the rods were considered. (2) The rods are one-dimensional lines with point dipoles spaced at regular intervals. When two rods are next to each other, the interval can be approximated by letting the distance between the two rods be a , where $a = 2 \times \text{radius of a rod}$.

With these simplifications, the problem resembles the well-known Ising problem in physics, which models ferromagnetism by representing the magnetic dipoles by point dipoles on a discrete lattice.

Next, the interaction potential energy can be calculated using the equation

$$u_{ij} = \frac{\mathbf{p}_i \cdot \mathbf{p}_j - 3(\mathbf{p}_i \cdot \hat{\mathbf{n}})(\mathbf{p}_j \cdot \hat{\mathbf{n}})}{r_{ij}^2} \quad (1)$$

where p_i is the dipole at the i^{th} point on the one-dimensional line representing rod 1, and p_j is the dipole at the j^{th} point on the one-dimensional line representing rod 2. If there are n points on a line, then the total dipole of each rod is $\mathbf{P} = n\mathbf{p}$, where \mathbf{p} is the dipole of each point.

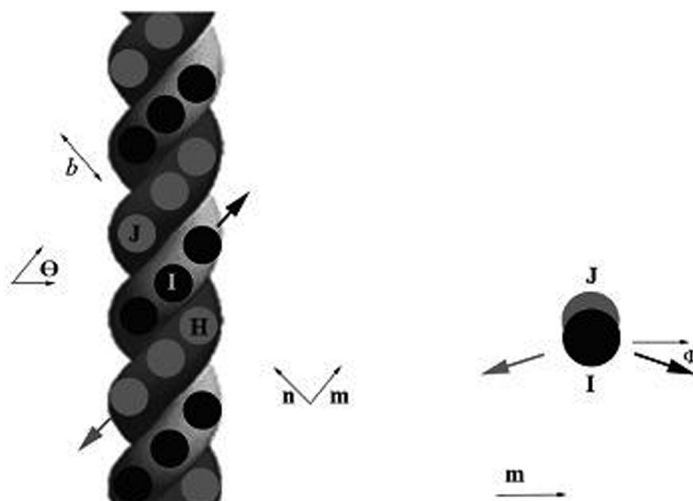


FIG. 10: Double-helix model. Two strands of point dipoles wind around each other. The dipoles are in the center of each strand. The dipoles in each strand point in opposite direction to the other strand. The strands are distance b apart. Panels H, I, and J represent dipoles. Θ is the helix angle; \mathbf{n} is the unit vector from dipole I to dipole J; \mathbf{m} is the unit vector direction along a strand; and Φ is the difference in angle between dipole I's direction and \mathbf{m} , and also between dipole J and \mathbf{m} .

If only nearest neighbor interactions is taken into account (as is often done in Ising model calculations also), then

$$u_{ij} = -\frac{p^2}{a^3} \quad (2)$$

and the total interaction energy of two adjacent straight rods is

$$U = -\frac{P}{a^3} \quad (3)$$

To model the two rods winding tightly around each other in a double helix, we begin with two dimensional lines at distance b apart. Modeling the pliability of the rods, the lines are allowed to wind around each other. To model the malleability of the rods, we allow b to be variable. For this calculation, assume the total dipole of each rod remains the same. We make

the simplification of periodic boundary conditions, so that one end of the helix is considered topologically connected to the other end. The spacing between the dipoles is chosen so that distance between nearest neighbor dipoles on opposite strands is minimized.

Assuming that z is the axis around which the double helix winds and ignoring the dipoles at the ends of the double helix, each dipole has three nearest neighbors: one in the strand diagonally above it, one in the strand diagonally below it, and one across from it on the horizontal plane.

On the right side of Figure 10, dipole I has the nearest neighbors dipole J and dipole H, as well as dipole K, which is behind it (not shown). The \mathbf{n} vector has a component in the y axis, if we define the y axis as being pointed into the page. On the left side of Figure 10, the \mathbf{n} axis points into the page. The dipoles

point at an angle Φ from the \mathbf{m} axis. Then the interaction energy between I and J is

$$u_{IJ} \sim - \frac{p^2 \cos 2\Phi}{b^3} \quad (4)$$

The interaction between I and H will have the same value.

The interaction energy between I and K is

$$u_{IK} = - \frac{p^2 \cos 2\theta}{b^3} \quad (5)$$

Assuming a rough approximation of $\theta = \Phi$ the total interaction energy between the two rods in the double helix is

$$U_{\text{int}} = (-3 \cos 2\theta) \frac{p^2}{b^3} \quad (6)$$

Examining the microscopy pictures, some values for b and θ can be approximated. If the diameter of the rods in the double helix configuration reduce to half its value in the straight rods $b = \frac{1}{2}\alpha$, the helix angle is $\theta = 30^\circ$. Then the total interaction energy is

$$U_{\text{int}} = -12 \frac{p^2}{a^3} \quad (7)$$

which is approximately 12 times lower than the interaction energy of the adjacent straight rod case. If the rods expel water and reduce in volume by a ratio of α , then

$$U_{\text{int-expel}} = -12\alpha \frac{p^2}{a^3} \quad (8)$$

An examination of Eq. 6 raises this question: Given that the smaller b is, the lower the potential energy, what prevents the strands from winding into thinner and thinner stands? One hypothesis is that the ball-like dipoles from the two strands initiate the winding process. Then they become compressed toward each other due to the electromagnetic attrac-

tion. If they are gels that initially hold liquid water, then they can expel the liquid water into the rest of the rods. They break free of the rest of the rod at some point and continue winding until they become a dry, compacted solid-like material in the middle. Meanwhile, the strands have filled with liquid water, creating a weak gel^{14,18} that does not have as strong a dipole nature, meaning that it will not continue winding after a certain point. An examination of Figure 4D, which shows a dark cylinder inside the double helix, with a more electron-translucent area outside, gives support to this hypothesis. The dark area is interpreted to mean the compacted dipolar ball-like structures, and the translucent area is interpreted to mean the weak gel filled with water that does not have as strong an electric field.

Some of the liquid water may also be expelled outside the structure. Figure 11 shows an AFM image taken 30 minutes after evaporation of the water droplet, and water can be seen outside the double-helix shape. This may be a picture of the water that was expelled, or it may be a picture of the surrounding water that has been restructured, perhaps due to the electrical fields that arise from the winding of the rods. Whether it is related to EZ water²⁰ is a topic for further investigation.

There is also another reason that the strands may have stopped winding and that it takes energy to stretch the rods:

$$\Delta U_{\text{total}} = \text{potential energy of stretching} + \Delta U_{\text{interaction}} \quad (9)$$

Systems move toward states of lowest free energy. The free energy of a state is $F = U - TS$; its value is dependent on temperature and entropy. Work is performed by a system when it moves to lower potential energy. Two rods will thus perform work when they wind into a double helix; they

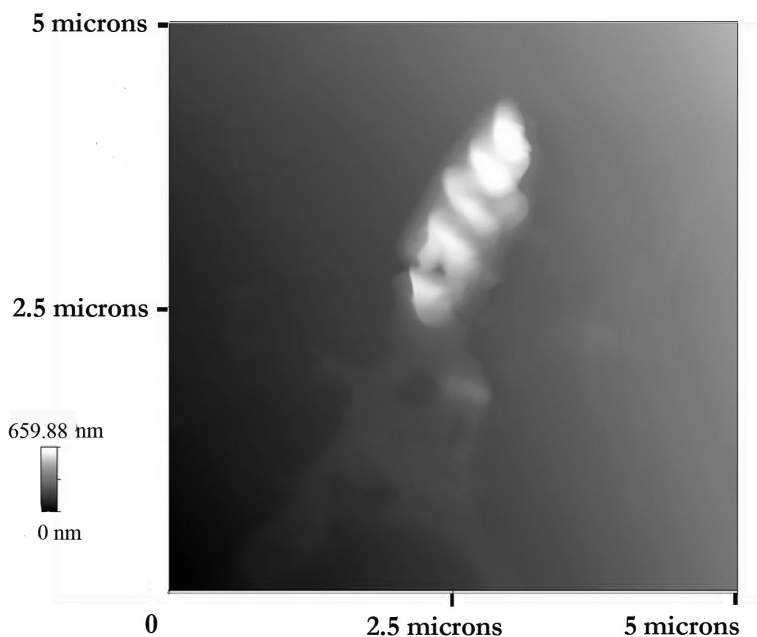


FIG. 11: AFM of double-helix rods: Taken 90 minutes after droplet laid out to dry on graphite. A trail of amorphous water structure can be observed at the lower end of the rod. It may be water expelled from the double helix, or it may be surrounding water restructured.

can increase the angular momentum of the surrounding water, and they can generate a temporary electromagnetic field.

D. Range of Structures

The stable water clusters display a wide range of structures. A partial selection of the wide variety of structures we see are presented in Figures 5D, 5E, and 5F. Closer examination of each picture shows that there are small ball-like structures making up these structures. Dipole-ball models are used in a variety of ways.^{24–27} Presented here is a coarse-grained model that can explain how these forms can self-assemble. This model consists of a ball with a dipole charge and an ambient material that is amorphous with adhesive attraction to the balls. Then, using the dipole–dipole

interaction, a wide range of structures that correspond to what we see is found. Dipoles have two energetically favorable configurations, antiparallel when next to each other, and parallel when placed end to end (Figure 12).

These balls can then self-assemble into a variety of energetically favorable configurations based on how each dipole wants to orient itself relative to its nearest neighbors. As shown in Figure 13A, ambient material flows into the middle forming a circle, and as shown in Figures 13B and 13C, into the inter-dipole area. The ambient material further helps to hold the structure and can serve as a buffer that keeps distance between dipoles. Figure 13A corresponds to the loop structure in Figure 5D; Figure 13B corresponds to the wreath structure in Figure 5E; and Figure 13C corresponds to

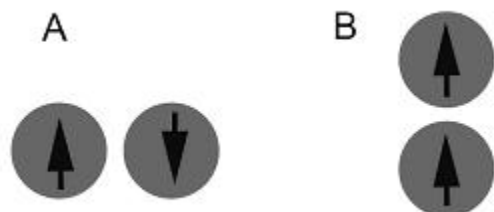


FIG. 12: Energetically favorable orientations of dipoles. **(A)** Dipoles prefer to align antiparallel when next to each other. **(B)** Dipoles prefer to align parallel when end to end.

the array structure in Figure 5F.

In his previous work, Lo used laser spectroscopy to image the breakup of larger stable water clusters in liquid water when shaken, and their subsequent growth when the liquid shaking stopped.⁸ This is an indication that the clusters were self-assembling in the liquid. The stable water clusters examined in the present study may have formed while in liquid or during the evaporation process.

IV. CONCLUSION

An examination of stable water clusters reveals surprising behavior when viewed in the context of conventional expectations of the states of matter in which water can exist. The data suggest that stable water clusters can bend, wind around each other, are malleable to pressure, are softer than rigid solids, and exhibit limited viscous flow. The results of this study suggest that we shift to a new soft-matter perspective, a perspective traditionally foreign to water science, to better understand stable water clusters. Almdal *et al.* has proposed one definition of a gel: (1) soft, (2) solid-like, and (3) exhibits two components, one of which is a liquid. Our data suggest that stable water cluster rods satisfy

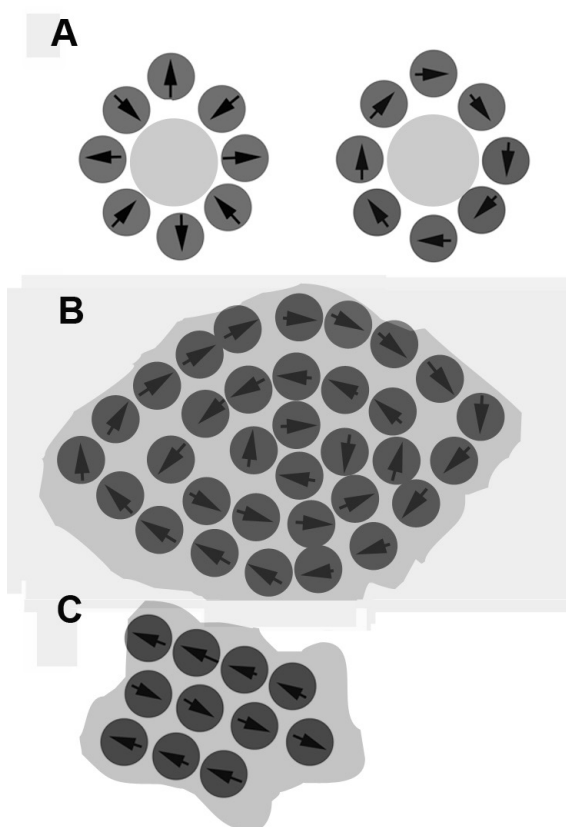


FIG. 13: Energetically favorable configurations for ball dipoles. The light-gray area represents ambient gel-like material. Panels **A**, **B**, and **C** correspond to Figs. 5D, 5E, and 5F, respectively. **(A)** Loop configuration with dipoles on outside, ambient material forming buffer in middle. **(B)** Wreath configuration. **(C)** Array configuration.

the first two conditions. Further investigation is required to determine whether stable water clusters exhibit the third condition. If they do, stable water clusters may be considered a gel. Stable water clusters are found in a number of different structural forms. One is a double-helix configuration, which suggests that stable water clusters rods are able to wind around each other. This can be modeled theoretically by assuming that the rods

are made of dipoles. The electromagnetic potential energy of the double helix configuration of the rods is found to be lower than the unwound rod configuration. The stable water clusters also form a number of other patterns, including arrays, loops, and wreaths. These structures are made of smaller, ball-like structures. A coarse-grained model based on dipolar ball-like structures exhibits self-assembly into the experimentally observed structures. Self-assembly at mesoscopic size scales occurs commonly in soft-matter systems. An understanding of the dynamical and structural behavior of stable water clusters can be arrived at within the context of the self-assembly of a soft-matter system.

ACKNOWLEDGMENTS

We would like to acknowledge David Gann for the myriad of ways he has supported this project. We would like to acknowledge Selim Senkan and Anusorn Seubsai of UCLA for assistance with the TEM.

REFERENCES

1. de Gennes P. Soft Matter (Nobel lecture). *Angewandte Chemie*. 1992;31:842-45.
2. de Gennes P. Soft matter: more than words. *Soft Matter*. 2005;1:16.
3. Jones R. *Soft condensed matter*. Oxford: Oxford Masters Series; 2002.
4. Lo SY. Anomalous State of Ice. *Modern Physics Letters B*. 1996;10:909-19.
5. Bonavida B, Gan XH. Induction and regulation of human peripheral blood TH1-TH2 derived cytokines by IE water preparations and synergy with mitogens. *Physical, Chemical and Biological Properties of Stable Water Clusters, Proceedings of the First International Symposium*. World Scientific Publishing Company; 1998.
6. Sinitsyn AP, Berson O, Lo SY. Effect of IE solutions on enzymes and microbial cells. *Physical, Chemical and Biological Properties of Stable Water Clusters, Proceedings of the First International Symposium*. World Scientific Publishing Company; 1998.
7. Lo SY, Geng X, Gann D. Evidence for the existence of stable water clusters at room temperature and normal pressure. *Phys Letts A*. 2009;373:3872-76.
8. Lo SY. Survey of IE clusters. *Physical, Chemical and Biological Properties of Stable Water Clusters, Proceedings of the First International Symposium*. World Scientific; 1998.
9. Dusek K and Patterson D. A transition in swollen polymer networks induced by intramolecular condensation. *J Polymer Sci Part A-2*. 1968;6:1209-16.
10. Shibayama M, Tanaka T. Volume phase transition and related phenomena of polymer gels. *Adv Polymer Sci*. 1993;109:1-62.
11. Kohl I, Bachmann L, Mayer E, Hallbrucker A, Loerting T. Water behaviour: glass transition in hyperquenched water? *Nature*. 2005;435:E1.
12. Loerting T, Giovambattista N. Amorphous ices: experiments and numerical simulations. *J Phys Condens Matter*. 2006;18:R919-77.
13. Almdal K, Dyre J, Hvidt S, Kramer O. Towards a phenomenological definition of the term 'gel'. *Polymer Gels and Networks*. 1993;1:5-17.
14. Nishinari K. Some thoughts on the definition of a gel. *Prog Colloid Polym Sci*. 2009;136:87-94.
15. Flory PJ. Gels and gelling process. *Faraday Discuss Chem Soc*. 1974;57:7-18.
16. Jordan Lloyd D, Alexander J. editor. *Colloid chemistry*. New York: Chemical Catalog

- Company; 1926.
17. Ross-Murphy S. Rheological characterization of gels. *J Texture Stud.* 2007;391–400.
 18. Ross-Murphy SB. Structure–property relationships in food biopolymer gels and solutions. *J Rheology.* 1995;39:1451–63.
 19. Zheng J, Pollack G. Long-range forces extending from polymer-gel surfaces. *Phys Rev E Stat Nonlin Soft Matter Phys.* 2003;68:031408.
 20. Pollack G. *The fourth phase of water: beyond solid, liquid, and vapor.* Ebner and Sons; 2013.
 21. Fuchs EC, Woisetschlager J, Gatterer K, Maier E, Pecnik R, Holler G, Eisenkolbl H. The floating water bridge. *J Physics D: Appl Phys.* 2007;40:6112–14.
 22. Del Giudice E, Preparata G, Vitiello G. Water as a free electric dipole laser. *Phys Rev Lett.* 1988;61:1085–88.
 23. Del Giudice E, Fuchs EC, Vitiello G. Collective molecular dynamics of a floating water bridge. *Water J.* 2010;2:69–82.
 24. Goyal A. Computer simulation studies of self-assembly of dipolar and quadrupolar colloid particles. UMI Dissertation Publishing; 2011.
 25. Schmidle H, Hall CK, Velev OD, Klapp SHL. Phase diagram of two-dimensional systems of dipole-like colloids. *Soft Matter.* 2012;8:1521–31.
 26. Pastor-Satorras R, Rubi JM. Particle-cluster aggregation with dipolar interactions. *Phys Rev E.* 1995;51:5994–6003.
 27. Adriani P, Gast A. A microscopic model of electrorheology. *Physics of Fluids.* 1988;31:2757–68.